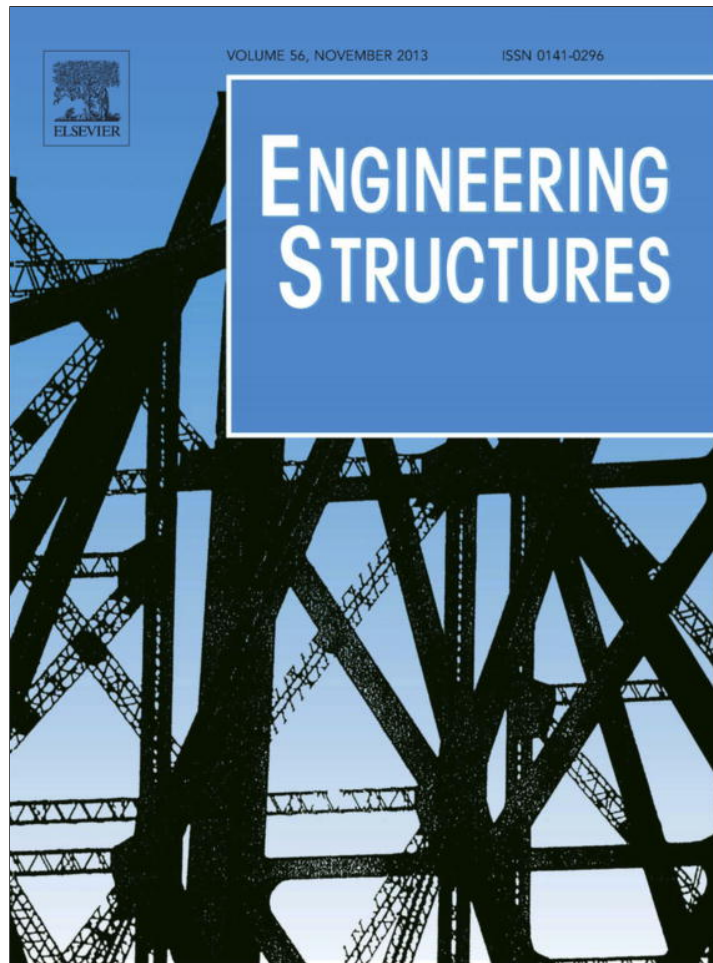


Provided for non-commercial research and education use.  
Not for reproduction, distribution or commercial use.

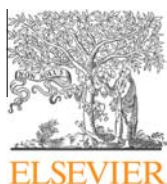


This article appeared in a journal published by Elsevier. The attached copy is furnished to the author for internal non-commercial research and education use, including for instruction at the authors institution and sharing with colleagues.

Other uses, including reproduction and distribution, or selling or licensing copies, or posting to personal, institutional or third party websites are prohibited.

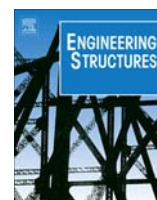
In most cases authors are permitted to post their version of the article (e.g. in Word or Tex form) to their personal website or institutional repository. Authors requiring further information regarding Elsevier's archiving and manuscript policies are encouraged to visit:

<http://www.elsevier.com/authorsrights>



Contents lists available at ScienceDirect

## Engineering Structures

journal homepage: [www.elsevier.com/locate/engstruct](http://www.elsevier.com/locate/engstruct)

## Long term behavior of FRC flexural beams under sustained load

Emilia Vasanelli <sup>a,1</sup>, Francesco Micelli <sup>a,\*</sup>, Maria Antonietta Aiello <sup>a</sup>, Giovanni Plizzari <sup>b</sup><sup>a</sup> University of Salento, Dept. of Engineering for Innovation, Via per Monteroni, 73100 Lecce, Italy<sup>b</sup> University of Brescia, Dept. of Civil Engineering, Architecture, Land and Environment, Via Branze 43, 25123 Brescia, Italy

## ARTICLE INFO

## Article history:

Received 24 July 2012

Revised 17 July 2013

Accepted 23 July 2013

Available online 12 September 2013

## Keywords:

Fiber reinforced concrete beams

Durability

Long term behavior

## ABSTRACT

Early applications of Fiber Reinforced Concrete (FRC) mainly concerned structural elements where the convenience of using short fibers was found in the possibility of substituting conventional reinforcement. However, FRC toughness can be conveniently introduced into the engineering practice with another perspective, to take advantage of the crack control for enhancing structural durability.

In this context, the research study presented herein shows the results of an experimental campaign aimed at investigating the influence of short fibers (steel and polyester) on the short and long-term behavior of Reinforced Concrete (RC) beams. The experimental program includes crack width and flexural displacement measurements as well as chemical tests, which gave evidence of the effectiveness of polymeric and steel fibers in improving long-term serviceability of RC beams. The results presented in the paper show that flexural displacements, crack widths and carbonation depth were reduced by the fibers addition.

© 2013 Elsevier Ltd. All rights reserved.

## 1. Introduction

Costs for maintenance and repair of conventional Reinforced Concrete (RC) buildings and structures have traditionally been an economic and social problem but, today, has also become a sustainability issue for the construction industry. Many RC structures deteriorate long before their design service life and it is estimated that the average service life of RC structures can be as short as several decades [1].

A possible solution of the problem is to invest in enhancing durability of new RC structures by using construction materials which would give perspective of a longer service life. In this context, the use of short fibers in concrete, in addition to conventional steel rebars, may be an effective way; in fact, fibers enhance the concrete toughness. The latter can prevent the occurrence of large cracks that allow water and contaminants to enter, causing corrosion of reinforcing steel or potential deterioration of concrete.

For these reasons, FRC may also be an effective design solution for structures exposed to aggressive environments. In fact, depending on the exposition class, the various international codes impose narrow limits on crack width in order to prevent corrosion of steel bars. The CEB FIP Model Code 1990 [2] and the Eurocode 2 [3] allow for a maximum crack width of 0.3 and 0.4 mm, respectively, that becomes smaller in aggressive environments [4]. ACI

Committee 222 [5] suggests a limit of 0.33 mm for exterior members and a limit of 0.41 for interior members; ACI Committee 224 [6] suggests crack widths ranging from 0.1 to 0.41 mm, depending on the exposition class.

In order to fulfill the code requirements, designers are asked to increase the reinforcement ratio and/or the section dimensions, thus leading to more expensive solutions. In this context, the use of FRC may be a good solution to reduce crack width without changing other, more expensive, design parameters.

Besides the reinforcement ratio, the bar size, the concrete properties, the cover thickness and, the load type (long or short term, cyclic or monotonic), when using FRC another design parameter influences the cracking process, namely the fracture toughness (ability to resist cracking), which strongly depends on the fiber type (material and geometry) and content as well as on the matrix properties. A well-established method to predict crack opening in RC/FRC members is still lacking in the literature. Analytical models have been proposed by some authors [7–10] but more experimental research is needed to validate the proposed formulations. In fact, only few experimental research on reinforced concrete beams quantitatively relate the crack development (width and spacing) to the fibers properties [7,8,11,12]. Results obtained show a considerable reduction of crack width by embedding fibers and this effect increases with higher volume dosage and lower reinforcement ratio. Oh [11] found a 45% reduction of crack width, under service loads, with a volume fraction of steel fibers equal to 2% and a reinforcement ratio equal to 65% of the balanced one. This effect was lesser pronounced in doubly reinforced beams where it was observed a reduction of crack width of about 25%. Tan et al. [8] also

\* Corresponding author. Tel.: +39 0832 297380; fax: +39 0832 297348.

E-mail address: [francesco.micelli@unisalento.it](mailto:francesco.micelli@unisalento.it) (F. Micelli).<sup>1</sup> Institute for Archaeological and Monumental Heritage (CNR-IBAM), Via per Monteroni, 73100 Lecce, Italy.

found a remarkable reduction of crack width that significantly depends on the fiber content; under service loads, with a reinforcement ratio equal to 62% of the balanced one, a crack width reduction up to 75% was observed in beams reinforced with a volume fraction of 2% of steel fibers.

Other works confirmed the effectiveness of fibers in reducing crack openings, analyzing the influence of fibers on tension stiffening [13–15].

The influence of fibers reinforcement on cracking behavior of RC beams under sustained loads is a topic almost unexplored. In fact, to the best knowledge of the authors, to date only the works of Tan et al. [8,16] are focused on this issue.

In the present research, the role of fibers in reducing crack widths of RC beams under service loads is investigated. To this aim 10 full scale beams, with and without fibers, were exposed to natural weathering under a sustained flexural load for a period of 17 months. During this period, the crack development of each beam (namely crack position, width and length) was monitored with a regular time scheduling. Eventually, some beams were unloaded and tested in laboratory for determining the mechanical behavior after exposure, the carbonation depth and the presence of chlorides. Three more beams were tested in short term loading condition and were used as control specimens.

## 2. Experimental program

A combined (mechanical and chemical) test protocol to evaluate the influence of fibers on durability of RC beams was adopted. The investigation of the long-term effects consisted of three different steps besides the material characterization. A first step was performed in the field, detecting the cracking evolution of the beams under service loads in exposure conditions. A second laboratory phase involved a four point bending test that were performed on beams up to the collapse. The final step consisted of durability tests aiming at determining the carbonation depth and the content of chlorides by colorimetric methods.

### 2.1. Specimen description and materials

Thirteen beams were poured, of which three were used as reference (laboratory beams) while the others were exposed to natural weathering under sustained load. One year after casting, the laboratory beams were tested (short term bending test) while the others were placed under two loading frames (Figs. 1a and 1b) at the exposure site. The supports position was designed in order to counterbalance the self-weight of each beam (Fig. 1b). The loading scheme of each beam is reported in Fig. 2 that shows a four



Fig. 1a. Exposed beam under the two loading frames (frame 1 and frame 2).

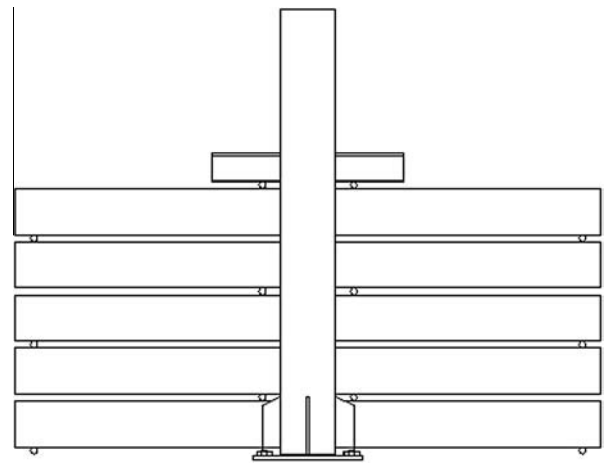


Fig. 1b. Details of the loading frame.

point bending condition with a span of 280 cm and a distance of 90 cm between the two loading points. The beams of frame 1 were unloaded after 17 months of exposure and transferred to the laboratory for flexural and durability tests. The beams of frame 2 are still exposed and monitored; they will be tested after a longer period.

Two different types of fibers were used: polyester fibers (Graminflex PE30 furnished by La Matassina Technology) and steel fibers (La Gramigna 060x30 furnished by La Matassina Technology). The aspect ratio (length/diameter) was 50 for steel fibers and 66 for polyester fibers, all other geometrical and mechanical properties of the short fibers as measured by the manufacturer are summarized in Table 1.

Three different concrete mixes were prepared: a reference mix without fiber reinforcement (TQ), a concrete mix with a volume fraction of 0.6% of steel fibers (ST) and a concrete mix with 0.9% of polyester fibers (POL). The fiber volume fractions were decided on the basis of results obtained by a previous research [18] considering the best compromise in terms of mechanical properties and workability of concrete. All the mixes had a water–cement ratio equal to 0.65, a cement type 32.5R II-A/LL [17] (Table 2.) and a workability class S5 [4]. Four cubes (150 × 150 × 150 mm) for each mix (TQ, ST and POL) were cast for quality control; the values of the compressive strength obtained after 28 days from casting are reported in Table 3. The compressive strength of ST mix was comparable to that of POL mix and both were slightly lower than the TQ strength. This was probably due to an higher content of entrapped air in the mix as it was found in a previous research carried out by authors [18]. Several authors agree that the influence of fibers on compressive strength is negligible [19–21].

Table 4 reports the average mechanical properties of longitudinal bars and stirrups adopted in the beams; they were measured according to UNI EN ISO 15630-1 [22] by testing three samples for each diameter.

The reinforced concrete beams were designed according to Italian Code [23], on the basis of the loading scheme reported in Fig. 2. The reinforcement ratio was chosen to have a bending failure of the beam, with concrete crushed after steel yielding of the tension bars. Vertical stirrups were also provided to prevent premature shear failure. Fig. 2 shows the geometry of the beams as well as the reinforcement details. Three tension and two compression bars having a diameter of 14 mm were used as longitudinal reinforcement while 8 mm stirrups were used as transverse shear reinforcement at a spacing of 140 mm that was reduced to 70 mm in the regions near the supports.

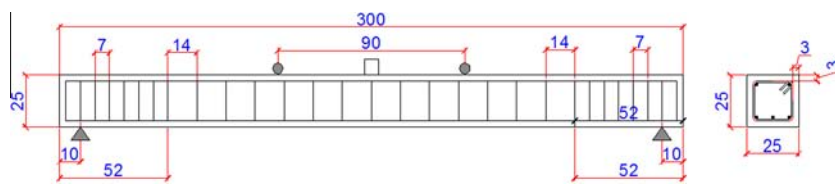


Fig. 2. Loading scheme and beams details (dimensions in cm).

**Table 1**  
Geometrical and mechanical characteristics of the fibers.

Type	Shape	Diameter ( $\mu\text{m}$ )	Length (mm)	L/D	Tensile strength (MPa)	Elastic modulus ( $\text{kN}/\text{mm}^2$ )
Steel	Hooked	600	30	50	>1150	210
Polyester	Waved	450	30	66	400–800	11.3

**Table 2**  
Composition of the concrete matrix.

	ST	POL	TQ
CEM 32.5R II-A/LL ( $\text{kg}/\text{m}^3$ )	300	300	300
Superplasticizer CRTV-L ( $\text{kg}/\text{m}^3$ )	1.59	2.50	1.77
Sand (0–4) ( $\text{kg}/\text{m}^3$ )	1028	1023	1037
Gravel (4–10) ( $\text{kg}/\text{m}^3$ )	704	701	710
Water/Cement ratio	0.65	0.65	0.65

**Table 3**  
Cubic compressive strength.

Beam	Average cube strength (MPa)	COV (%)
TQ	25.8	4
ST	21.4	8
POL	23.2	8

**Table 4**  
Mechanical properties of the steel rebars.

Materials	Diameter (mm)	Yield strength (MPa)	Ultimate strength (MPa)	Elongation at rupture (%)
Longitudinal bars	14	520	614	12.2
Stirrups	8	567	600	4.8

2.2. Field exposure measurements and site conditions

The exposure site is located in Brindisi (Southern Italy), in an industrial area at a distance of 600 m from the sea coast. The most important climatic factors, which may affect the time to corrosion initiation of steel bars, are the relative humidity and the presence of chlorides in the air. Climatic conditions at the test site were continuously registered during the exposure time.

As mentioned above, the exposed beams were positioned under two loading frames where five beams were piled up; they were loaded by means of a screw jack (Figs. 1a and 1b) with the same loading scheme used for bending test in laboratory (Fig. 2). In order to reproduce service conditions, the load applied during the exposure period was equal to 50 kN which was about 50% of the design ultimate load. Two load cells were placed under the screw jacks to monitor the applied load periodically. A data acquisition system was used to monitor the load variations due to relaxation effects of the loading system; for this reason, the beams were often reloaded in order to maintain the initial value of 50 kN.

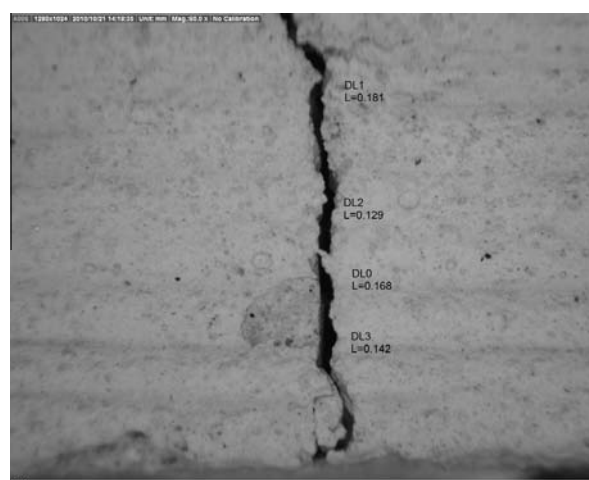


Fig. 3. Digital microscope image.

During the exposure period, measurements of crack width, depth and position were made on each beam. During the first 9 months of exposure, crack widths were measured by means of an optical scale loupe, with a precision of 0.05 mm. Afterwards, an handheld digital microscope with 200 $\times$  magnification was used. The crack widths was measured along each beam at the bottom of its tension edge. An example of digital image of cracks with their width is reported in Fig. 3.

2.3. Bending tests

The laboratory beams (TQ-L, ST-L and POL-L) and exposed beams of frame 1 (TQ1-E, ST1-E, ST2-E, POL1-E, POL2-E) were tested in bending up to failure by adopting the loading scheme of Fig. 2. Deflections at mid-span and at quarter points of the beams were measured during the test by means of three Linear Variable Differential Transducers (LVDTs) with a stroke of 50 mm. Tests were performed under load control; a load cell having a capacity of 30 ton was used to measure the applied force. The crack pattern of the exposed beams (number of cracks, crack widths and crack lengths) was recorded at five load steps: Step 1 = 20 kN; Step 2 = 30 kN; Step 3 = 50 kN; Step 4 = 80 kN; Step 5 = 100 kN. The crack widths were measured at the bottom of the tension edge of each beam by means of a digital microscope with a magnification up to 200 $\times$ .

2.4. Durability tests

After bending tests, the exposed beams were cut along their length and durability tests were carried out. In particular, the carbonation depth and the chloride penetration were detected on the split sections of each beam. The carbonated depth was assessed by a colorimetric method, based on the drop of PH at the carbonation front [24]. A phenolphthalein solution was sprayed on one of the two split sections of each beam. The depth of the carbonation front was measured along each beam, on its tension side, between cracks and at cracked sections. In particular, only cracks formed in the constant moment portion of the beams (between the two loading points) were analyzed in order to separate the flexural/shear interaction effects. At the cracked sections, the carbonation depth was measured along the crack direction; in particular, since the carbonation front had an irregular profile, three measures were taken to calculate an average value of the carbonation depth.

A colorimetric method was also used to determine the presence of free chlorides in concrete. The method is based on spraying silver nitrate aqueous solution (0.1 M AgNO<sub>3</sub>) on the concrete fractured surfaces: the dark colored area corresponds to a chloride-free concrete (Cl<sup>-</sup> less than 0.0012% by weight of concrete) while the

pink-colored area corresponds to a chloride-penetrated concrete [25].

3. Experimental results and discussion

3.1. Field exposure results

Air temperature, relative humidity and wind rate per day were provided by means of a meteorological station of ARPA Puglia (Agency for ambient prevention and protection of the local district). According to EN 206-1 [4], the site belongs to the exposition class XC3 for corrosion induced by carbonation, and to the exposition class XS1 for corrosion induced by chlorides.

Figs. 4a and 4b exhibit the average crack width vs. time, as measured between the two loading points of each beam of frames 1 and 2, respectively. Tables 5 and 6 report the mean numerical values. It should be observed that the crack widths measured on FRC beams were lower than those measured on TQ beams and that this effect increased with time. In fact, the crack width of FRC beams (ST and POL) seems to be stabilized after 10 months of exposure, while in TQ beams the crack width continued to grow

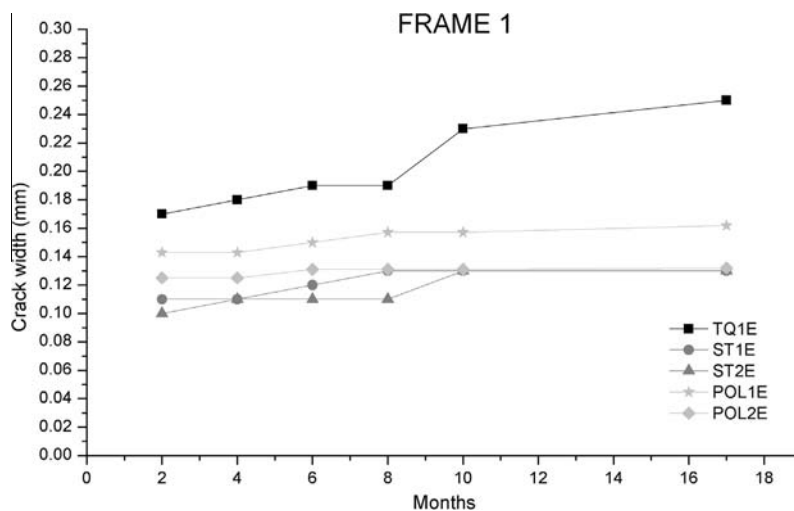


Fig. 4a. Average crack width vs. time measured on exposed beams of frame 1.

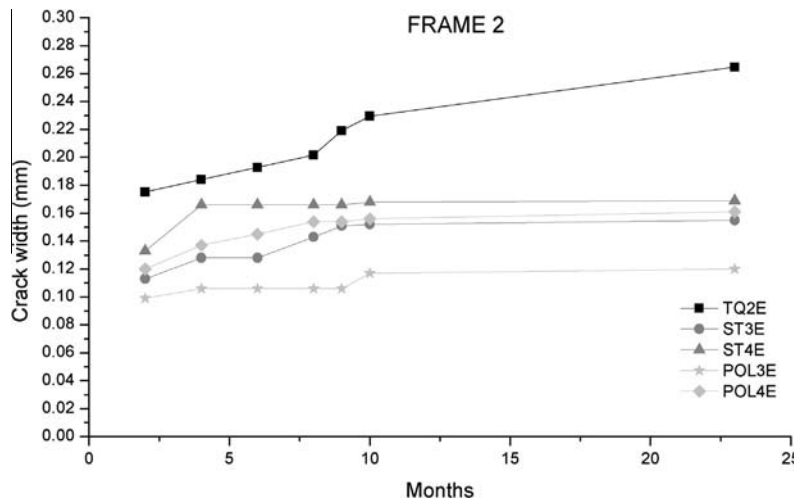


Fig. 4b. Average crack width vs. time measured on exposed beams of frame 2.

**Table 5**  
Average crack width of beams in frame 1.

Months	TQ1-E	ST1-E	ST2-E	POL1-E	POL2-E
2	0.17	0.11	0.10	0.14	0.13
4	0.18	0.11	0.11	0.14	0.13
6	0.19	0.12	0.11	0.15	0.13
8	0.19	0.13	0.11	0.16	0.13
10	0.23	0.13	0.13	0.16	0.13
17	0.25	0.13	0.13	0.16	0.13

**Table 6**  
Average crack width of beams in frame 2.

Months	TQ2-E	ST3-E	ST4-E	POL3-E	POL4-E
2	0.18	0.11	0.13	0.10	0.12
4	0.18	0.13	0.17	0.11	0.14
6	0.19	0.13	0.17	0.11	0.15
8	0.20	0.14	0.17	0.11	0.15
9	0.22	0.15	0.17	0.11	0.15
10	0.23	0.15	0.17	0.12	0.16
23	0.26	0.16	0.17	0.12	0.16

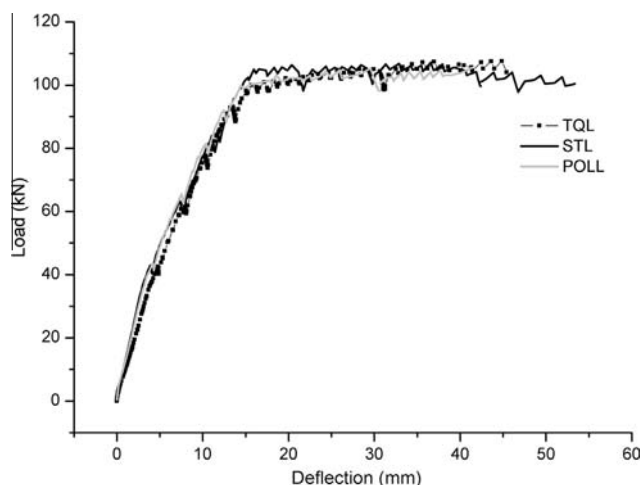


**Fig. 5.** Load-deflection behavior of laboratory beams.

**Table 7**  
First cracking load, steel yielding load and ultimate load of laboratory beams.

Beam	First cracking load (kN)	Steel yielding load (kN)	Ultimate load (kN)
TQ-L	11.19	84.24	107.62
ST-L	12.79	91.43	107.12
POL-L	9.99	88.03	105.52

**Table 8**  
Mid-span deflections (mm) at step 1–5 and at failure of laboratory beams.

Beam	STEP 1 (20 kN)	STEP2 (30 kN)	STEP3 (50 kN)	STEP4 (80 kN)	STEP5 (100 kN)	Ultimate deflection
TQ-L	2.27	3.23	5.93	11.20	17.18	45.42
ST-L	1.67	2.43	5.16	10.46	14.83	53.36
POL-L	1.70	2.60	5.47	10.12	14.44	41.38

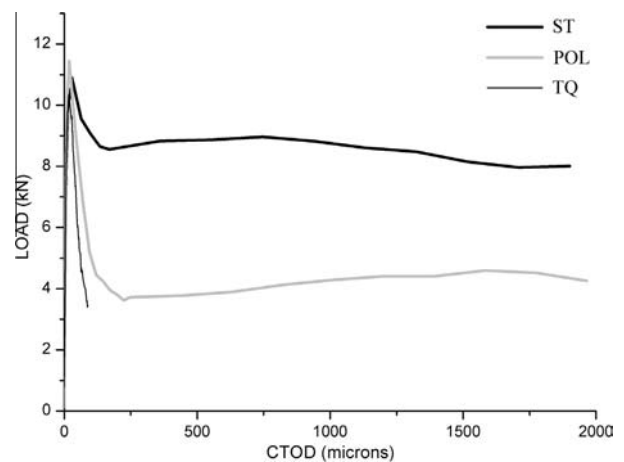


**Fig. 6.** Fracture test results of ST, POL and TQ notched beams.

during the exposure time. In particular, between the tenth and the 17th month of exposure, it was measured an increment of average crack width of 8% in TQ1-E beam, and of 13% in TQ2-E beam, while no significant increase of crack width was observed in FRC beams. Thus, the presence of fibers seems to help in reducing the long-term crack growth, as found by Tan et al. [8,16]. The causes of this behavior may be manifold. It has been proved that the crack width in concrete is affected by the loading time and this aspect has also been considered by the Codes [2,3]. In particular, the effect of time on crack width can be regarded as the sum of two components: one is related to free shrinkage of concrete and is independent on the applied load; the second is due to delayed strains in concrete caused by the presence of a sustained load. Recent studies have shown that the presence of fibers may reduce the creep strains and consequently crack widths especially for low load levels [26]. An analytical prediction of crack width using different code's formulations has been carried out by the authors [27] for short and long term loading conditions: in the research it has been evidenced that the codes predicted well the crack widths of plain concrete beams under long term loading while the FRC formulation need to be revised considering the influence of fibers in reducing the creep coefficient.

It has to be pointed out that, despite the higher modulus of steel fibers, steel and polyester fibers had quite the same effect on the cracking behavior of the beams. In fact, the final values of the average crack widths of POL and ST beams were not significantly different: POL beams of frames 1 and 2 had a mean crack width of 0.15 mm and 0.14 mm, respectively, while ST beams of frames 1 and 2 had a mean crack width of 0.13 mm and 0.16 mm, respectively.

This was observed also in the short term bending tests performed on the same beam typologies in a previous research [28]. It is in the opinion of the authors that the presence of stirrups, influencing the crack spacing value, had in part limited the effectiveness of steel fibers in reducing crack widths. Probably, if the stirrups were not present between the loading points of the beams,

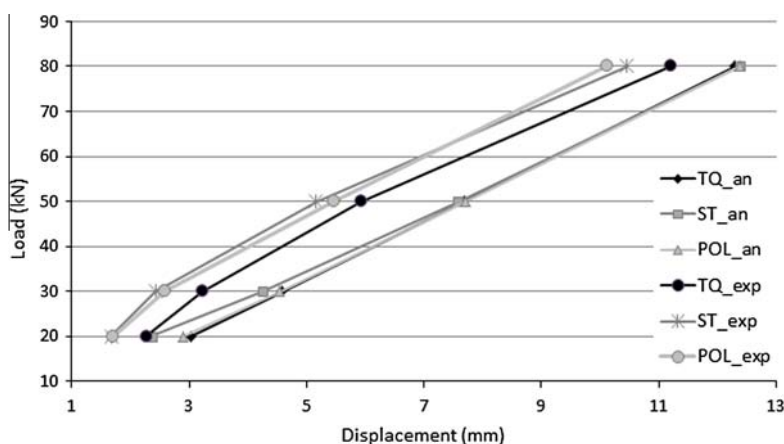


Fig. 7. Analytical and experimental Load-Deflection curves in short term loading condition.

a lower crack spacing value in ST beams would be observed compared to POL beams, causing lower crack openings.

### 3.2. Bending test results

#### 3.2.1. Load-deflection behavior – laboratory beams

As expected, all the tested beams collapsed by concrete crushing after yielding of tensioned steel bars. Fig. 5 shows the load-displacement curves of laboratory beams; the displacement was measured at mid-span by using LVDTs. It should be observed that the flexural behavior of FRC-L and TQ-L laboratory beams was very similar and that a typical pseudo bi-linear curve was obtained.

Table 7 reports the first cracking load, the load at yielding of longitudinal steel tensioned bars (Steel Yielding Load) and the ultimate load for each laboratory beam. The influence of fibers on the bearing capacity of the beams seems to be negligible. A little increment of first cracking load (almost 14%) and steel yielding load (almost 8%) was found only in the case of ST beams as compared to TQ beam. In Table 8, the mid-span deflection of the laboratory beams, as measured at each loading step, is reported; it can be observed that deflections of FRC beams were lower than those of TQ beam at all the load steps investigated (the stiffness increase due to fibers was much evident immediately after cracking – at step 1, equal to 26%, and after yielding of steel bars – at step 5, equal to 14%). In fact, the post cracking residual strength of FRC provided an increase of tension stiffening, as compared to plain concrete; this effect is more relevant just after cracking, when the plain concrete contribute in tension is drastically reduced, and after yielding of steel bars, when the sudden increase of steel deformability is mitigated by the presence of fibers. Steel and polyester FRC beams behaved similarly, despite of the differences obtained from results of fracture tests (Fig. 6), fully described in [18]. As was found by other authors [11,8] the effect of fibers is more appreciable when the reinforcement ratios are lower than the balanced one: in such

a situation the difference between steel and polyester fibers could be more relevant.

An analytical prediction of the beam deflection under short term loading has been carried out using the new Model Code for-

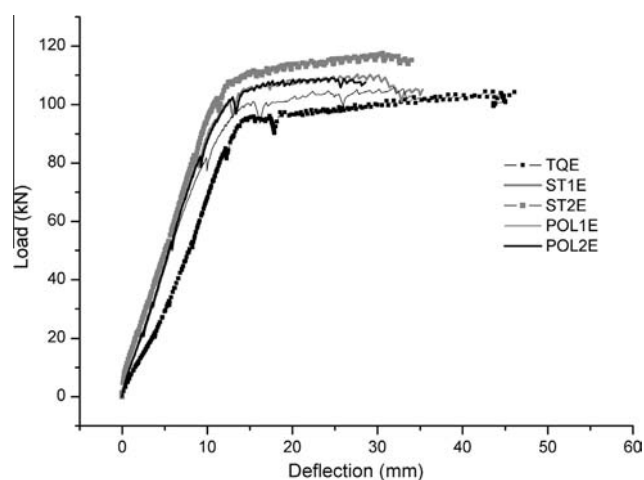


Fig. 8. Load-deflection behavior of exposed beams.

Table 9  
Steel yielding load and ultimate load of exposed beams.

Beam	Steel yielding load (kN)	Ultimate load (kN)
TQ1-E	88.33	104.42
ST1-E	91.93	110.32
ST2-E	92.93	117.41
POL1-E	87.84	105.82
POL2-E	90.23	109.12

Table 10  
Mid-span deflections (mm) at step 1 to 5 and at failure of exposed beams.

Beam	STEP 1 (20 kN)	STEP2 (30 kN)	STEP3 (50 kN)	STEP4 (80 kN)	STEP5 (100 kN)	Ultimate deflection
TQ1-E	3.54	5.25	7.93	11.48	28.99	46.10
ST1-E	2.27	3.5	5.58	8.64	12.14	35.3
ST2-E	1.71	2.81	5.06	8.27	10.86	34.0
POL1-E	2.07	3.36	5.64	9.55	14.49	34.9
POL2-E	2.21	3.49	5.55	8.88	12.35	28.57

mulations [29]. In particular, the load–deflection curve has been estimated for load levels up to steel bars yielding for both FRC and plain beams. In order to model the contribute of fibers in tension the constitutive  $\sigma$ – $\varepsilon$  law proposed in MC2010 was simplified considering a constant stress value  $f_{Fts}$  in the range between the first cracking strain ( $\varepsilon_p$ ) and the serviceability limit strain ( $\varepsilon_{sls}$ ). The values of  $f_{Fts}$  for POL and ST concrete were calculated starting from experimental results obtained on notched beam, fully described in [18,27]. The code's prediction shows a negligible reduction in mid-span deflection due to fibers: in particular, the POL and TQ beam analytical curves are almost overlapping due to the low  $f_{Fts}$  value of polyester fiber reinforced concrete (Fig. 7). The major fiber contribute in reducing the mid-span deflection was at first loading steps (20–30 kN) as evidenced also by experimental results. The code prediction furnished precautionary mid-span deflection values compared to experimental results, especially when referring to FRC beams. The average scatters between experimental and analytical results were 29%, 45% and 52% respectively for TQ, ST and POL beams, considering all the loading steps investigated.

### 3.2.2. Load–deflection behavior – exposed beams

Fig. 8 shows the load–displacement curves of exposed beams. Table 9 reports the load at yielding of steel bars (Steel Yielding Load) and the ultimate load values for each exposed beam. The presence of fibers provoked a slight increment in yielding loads compared to those obtained for TQ beams. POL1-E beam had a yielding load lower than that of TQ1-E; however, during the test it was observed that the POL1-E beam had the upper face not perfectly planar, probably causing some eccentricity during loading and, consequently, an early yielding of steel bars in tension. The presence of fibers allowed an increment in the ultimate load up to 12% for ST2-E with respect to TQ1-E. This effect was not observed in laboratory beams; probably the higher damage level of TQ1-E beam due to long term loading could explain this effect.

Table 10 reports the deflections at mid-span of exposed beams, measured at each load step up to failure; one should observe that FRC beams were considerably stiffer than TQ beam at all the loading steps investigated while, in laboratory beams, this effect was not so evident. This result evidences that the presence of fibers strongly affects the long term behavior of RC beams under sustained load. To better understand the role of fibers in reducing creep effects, the load–deflection curves of laboratory and exposed beams are compared in Figs. 9a, 9b and 9c. Up to 50 kN (load applied during exposure), all the exposed beams had lower stiffness as compared to the corresponding laboratory beams. As the load increased, all the exposed FRC beams reached the same stiffness (even higher) of the corresponding laboratory beam; while the TQ1-E beam reached the load of 100 kN at very high deflection, compared to TQ-L.

The benefic role of fibers in reducing delayed deflections is not evidenced by analytical prediction. In fact, considering the MC 2010 formulation for FRC and plain concrete taking into account the effect of time (shrinkage and creep), the displacements predicted for FRC and plain beams are quite the same in contrast with the experimental results (Fig. 10). Probably the creep coefficient formulation has to be revised in order to take into account the beneficial effect of the fibers. This aspect has been pointed out by the authors also for crack width estimation [27] and has been evidenced by other authors [26], thus more research is needed to correctly quantify the creep coefficient in presence of fibers.

All the exposed beams failed in bending with concrete crushing after steel yielding, but TQ1-E beam showed a more extensive concrete damage as compared to FRC beams. This is quite evident in Figs. 11 and 12, where the final cracking pattern of TQ1-E and

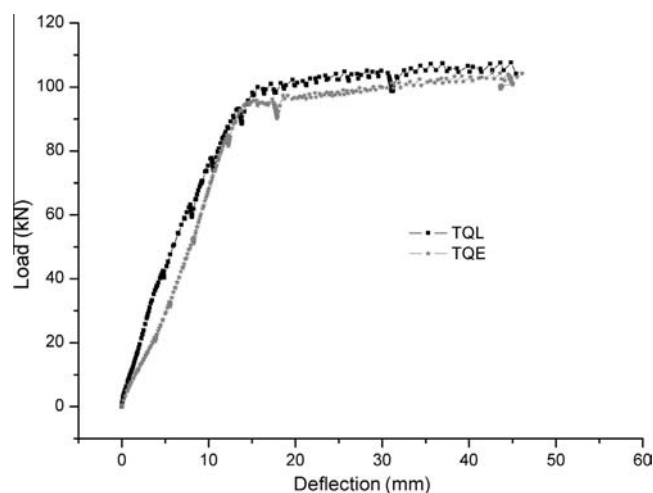


Fig. 9a. Comparison between load–deflection curves of TQ-L and TQ1-E beams.

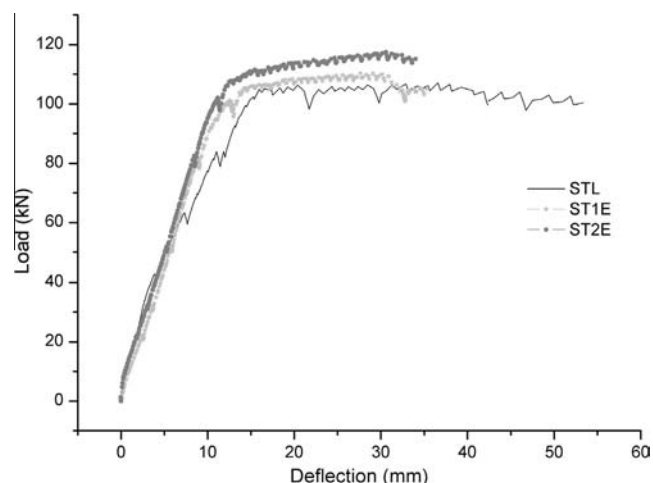


Fig. 9b. Comparison between load–deflection curves of ST-L and ST1,2-E beams.

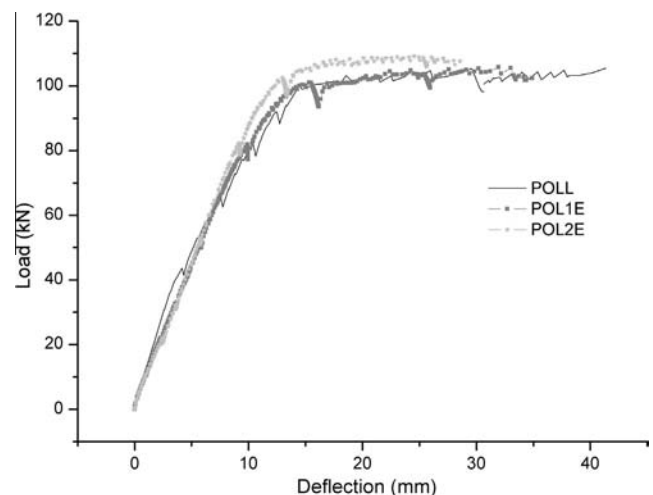


Fig. 9c. Comparison between load–deflection curves of POL-L and POL1,2-E beams.

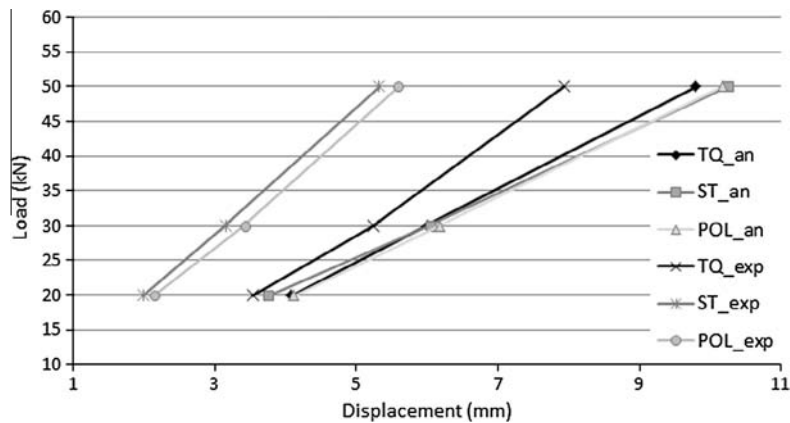


Fig. 10. Analytical and experimental Load-Deflection curves in long term loading condition.

ST1-E beams is shown (the other FRC beams had a failure mode very similar to that of ST1-E beam) [16].

### 3.2.3. Cracking behavior

Crack width measurements were made on exposed beams during the bending tests (Fig. 13 that refers to the average crack widths calculated in the beam portion with a constant bending moment). One should observe that the crack width was lower in FRC beams than in the TQ beam. The POL2-E beam behaved very similar to ST beams while POL 1-E beam differed from the other FRC beams, approaching the TQ beam behavior, especially in the last loading steps. As before mentioned (Section 3.2.1), POL1-E beam had the upper face not perfectly planar, probably causing

some eccentricity during loading and, consequently, wider crack openings. Thus, in the following, POL1-E beam was not considered and the expression “FRC beams” refers to ST beams and POL2-E beam.

At 20 kN, TQ1-E beam showed an average crack opening equal to 0.24 mm, very similar to the average crack opening value measured after 17 months of exposure (3.1). In FRC beams the average crack width at 20 kN was about 0.10 mm, namely 23% less than that measured on the exposure site (0.13 mm). Thus, it can be observed that the presence of fibers helped in reducing residual crack openings after unloading of the beams. Another important feature is the difference in the cracking behavior between TQ and FRC beams, after yielding of steel bars (step 5: 100 kN). Looking at the curves shown in Fig. 15, it can be seen that the slope of the TQ1-E curve become steeper starting from 80 kN, while the slope of the FRC curves remained quite constant up to 100 kN. At the last load step it was observed a reduction in crack width of about 56% due to fibers. This reflects the attitude of fibers in reducing tensile stresses of steel bars (tension stiffening) even at high values of crack openings, when the contribute of plain concrete had vanished.

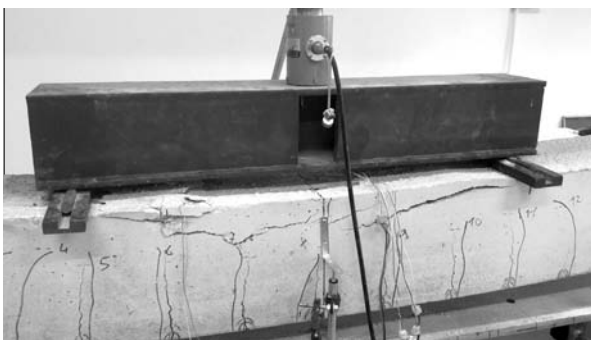


Fig. 11. Final crack pattern (at failure) of TQ1-E beam.

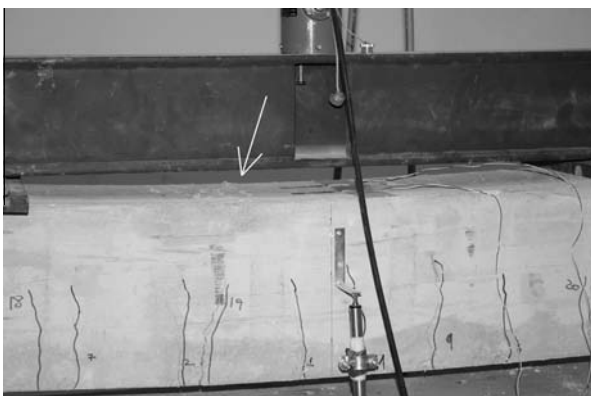


Fig. 12. Final crack pattern (at failure) of ST1-E beam.

### 3.3. Durability test results

Fig. 14 exhibits the average values of carbonation depths measured over the entire length of the beams, on their tension edge. The measurements were made every 300 mm along the longitudi-

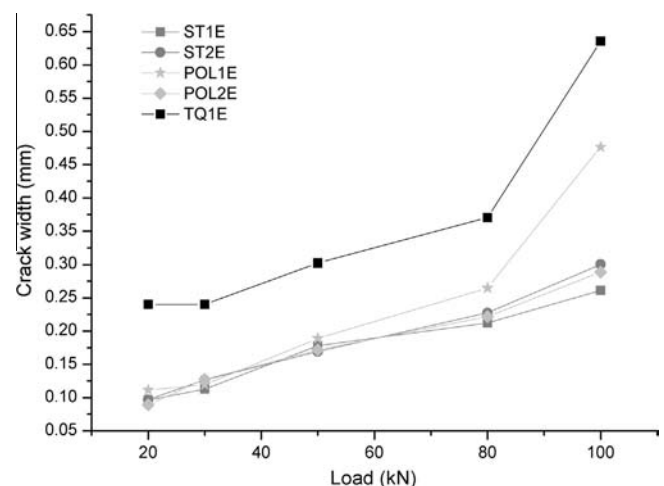


Fig. 13. Average crack with-load curves of exposed beams.

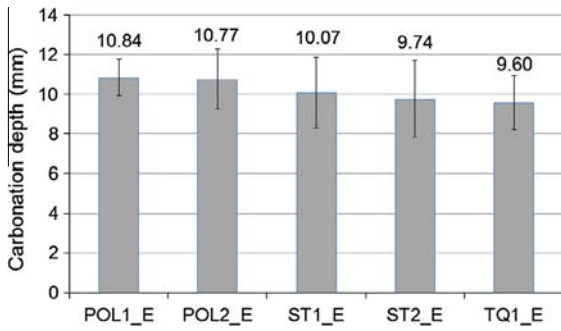


Fig. 14. Average carbonation depth as measured in uncracked regions.

and the carbonation depths reported in Figs. 14 and 15, the  $K$  coefficient can be calculated for each beam, as reported in Table 11.

Although several studies have been devoted to the deterioration of carbonated concrete, a few studies discuss the effect of crack opening on the ingress of carbon dioxide [30]. The possibility of using Eq. (1) as a crack age indicator is still a matter of research [31,32]. Some authors [33] agree that, referring to the carbonation process, the basic interrelations given for uncracked concrete are also valid in cracked regions. Thus, Eq. (1) was used to calculate  $K$  at cracked sections; the average value obtained for each beam is given in Table 11. Two considerations can be made: first, the  $K$  values at cracked sections were higher than those at uncracked regions; this means that carbonation can penetrate much faster into cracks than it does through uncracked concrete. Secondly, the coefficients of carbonation of FRC beams at cracks were lower than that of TQ beam.

Knowing the  $K$  values for each beam, a rough prevision of the time needed for  $CO_2$  to reach steel bars can be made (Table 11). It can be observed that the presence of fibers contribute in doubling the time to reach bars in presence of cracks, with respect to plain concrete. Thus on the basis of these experimental results the life cycle of an FRC flexural element seems to be almost doubled. This is of great interest if compared to the extra costs due to the addition of fibers (15–25%).

From colorimetric test, no chlorides (<0.0012% by weight of concrete) were detected on concrete surface for all the beams investigated. This is probably due to the short time of exposure in relation to possible chlorides ingress and to the quite high distance from the sea.

4. Conclusions

A research study was carried out to evaluate the role of fiber reinforcement in RC beams subjected to flexural loads with reference to long-term effects and cracking behavior under service conditions. A new combined test-protocol was presented, including in-field monitoring, laboratory mechanical tests and chemical measurements (durability tests) after exposure and flexural testing.

From experimental results obtained during the exposure period, the following remarks can be highlighted:

- the crack width measured on FRC beams were lower than those measured on plain concrete beams. This effect becomes more evident under sustained loads; in fact, the crack width of FRC beams (ST and POL) seems to stabilize after 10 months of exposure, while those of TQ beams continued to grow during the exposure time;
- steel and polyester fibers had quite the same effect on the cracking behavior of the beams. It is in the opinion of the authors that the presence of stirrups, influencing the crack spacing value, had in part limited the effectiveness of steel fibers in reducing crack widths.

nal axis. All the results were analyzed using the one way analysis of variance (ANOVA) in order to evaluate the effective influence of the presence of fibers and fiber type on the carbonation depth. Results showed that at 0.05 level of significance, the population means were not very different, evidencing that fibers did not affect in great extent the permeability of the matrix to  $CO_2$  when the matrix is uncracked.

Carbonation depth was also measured at cracked sections, making three measures on the carbonation front. In Fig. 15, the average values of the carbonation depth, measured at each crack section (in the constant moment portion of the beams), are reported. It can be observed that the average values of carbonation depth measured on FRC beams were from 24% to 36% lower than that of TQ beam, evidencing the attitude of fibers in reducing crack width, resulting in lower carbonation depths.

It is well known that, in uncracked concrete, the carbonation depth ( $D$ ) is related to the concrete exposure time to  $CO_2$  ( $t$ ), by the following equation:

$$D = Kt^{0.5} \tag{1}$$

where  $K$  is the carbonation coefficient. Therefore, by applying Eq. (1) to the case study, considering an exposure time of 17 months

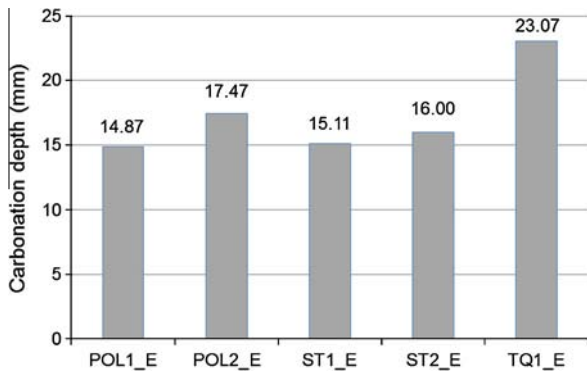


Fig. 15. Average carbonation depth as measured at the cracked sections.

Table 11 Carbonation coefficients ( $K$ ) and estimated time to reach steel bars ( $T$ ) for uncracked and cracked concrete.

Beam	$K$ (mm/year <sup>0.5</sup> )		$T$ (years)	
	Uncracked concrete	Crack section	Uncracked concrete	Crack section
TQ1-E	8.06	19.38	13.8	2.4
ST1-E	8.46	12.69	12.6	5.6
ST2-E	8.18	13.44	13.4	5
POL1-E	9.11	12.49	10.9	5.8
POL2-E	9.05	14.67	11.0	4.2

On the basis of results obtained from laboratory bending test, the following conclusions can be drawn:

- reinforced beams after exposure with respect to plain concrete beams (this effect an increment in the ultimate load was observed in steel fiber was not observed in laboratory beams);
- FRC exposed beams were considerably stiffer than plain concrete exposed beam; in laboratory beams this effect was not so evident;
- after yielding of steel bars, it was observed a significant reduction of crack width, evidencing the enhanced tension stiffening of FRC.

From these remarks it can be pointed out a strong influence of fibers on long term loading effects. The causes of this behavior may be manifold. Both the free shrinkage and the creep strains in concrete may be affected by the presence of fibers, thus more experimental research is needed to quantify in which extent the fibers influence the two mentioned aspects.

From durability tests results, it was observed that:

- fibers did not affect significantly the permeability of the matrix to CO<sub>2</sub> when the matrix is uncracked;
- the average value of carbonation depth measured on FRC beams in the cracked sections was remarkably lower than that of TQ beam;
- a rough prevision of the time needed for CO<sub>2</sub> to reach steel bars was determined, evidencing that, in cracked matrices, the presence of fibers seems doubling the time to have a CO<sub>2</sub> attack to steel reinforcement, compared to plain concrete. On the basis of these experimental results the life cycle of an FRC flexural element seems to be almost doubled. This is of great interest if compared to the extra costs due to the addition of fibers (15–25%).

The progress of the research work, namely monitoring and testing of the remaining exposed beams, will contribute to extend the database allowing more reliable design indications.

## Acknowledgements

A special acknowledgement goes to CTG Italcementi Group of Brindisi (Italy) for their valuable help in performing the experiments. The authors are also grateful to La Matassina Technology s.r.l. for providing all the fibers.

## References

- [1] Ahmed SFU, Mihashi H. A review on durability properties of strain hardening fiber reinforced cementitious composites (SHFRCC). *Cem Concr Compos* 2007;29:365–76.
- [2] CEB (Comite Euro-International du Beton). CEB-FIP Model Code 1990 *Bullettind'Information*, No. 203–205, Thomas Telford, London, UK; 1993. 437pp.
- [3] Eurocode 2. Design of concrete structures – Part 1–1: General rules and rules for buildings. EN 1992-1-1; 2004.
- [4] UNI EN 206-1. Concrete – specification, performance, production and conformity. Italian Board of Standardization (UNI); 2001.
- [5] ACI Committee 222. Corrosion of metals in concrete. *ACI J* 1985;82(1):3–32.
- [6] ACI Committee 224. Control of cracking of concrete structures. ACI Special Publication 224R-01.
- [7] Vandewalle L. Cracking behavior of concrete beams reinforced with a combination of ordinary reinforcement and steel fibers. *Mater Struct* 2000;33:164–70.
- [8] Tan KH, Paramasivam P, Tan KC. Cracking characteristics of reinforced steel fiber concrete beams under short and long-term loadings. *Adv Cem Mater* 1995;2:127–37.
- [9] Leutbecher T, Fehling E. Crack width control for combined reinforcement of rebars and fibres exemplified by ultra-high-performance concrete. In: fib task group 8.6 "Ultra high performance fibre reinforced concrete – UHPFRC" 2008, Varenna; 2008.
- [10] Chiaia B, Fantilli AP, Vallini P. Crack patterns in reinforced and fiber reinforced concrete structures. *Open Constr Build Technol J* 2008;2:146–55.
- [11] Oh BH. Flexural analysis of reinforced concrete beams containing steel fibers. *J Struct Eng* 1992;118:2821–36.
- [12] Balazs GL, Kovacs I. Effect of steel fibers on the cracking behaviour of RC members. In: Proceedings of 6th RILEM symposium on fiber-reinforced concretes – BEFIB 2004, 20–22 September 2004, Varenna, Italy; 2004.
- [13] Abrishami HH, Mitchell D. Influence of steel fibers on tension stiffening. *ACI Struct J* 1997;94:769–75.
- [14] Bishoff PH. Tension stiffening and cracking of steel fiber reinforced concrete. *J Mater Civ Eng* 2003;March–April:174–82.
- [15] Minelli F, Tiberti G, Plizzari G. Durability and cracking in fibrous R/C elements: a broad experimental study. *Atti del Convegno Le Nuove Frontiere del Calcestruzzo Strutturale, Università degli Studi di Salerno – ACI Italy*, 22–23 April; 2010 [Chapter].
- [16] Tan KH, Saha MK. Ten-year study on steel fiber-reinforced concrete beams under sustained loads. *ACI Struct J* 2005;102-3:472–80.
- [17] UNI EN 196-1. Cement – Part 1: composition, specifications and conformity criteria for common cements. Italian Board of Standardization (UNI); 2007.
- [18] Vasanelli E, Micelli F, Aiello MA, Plizzari G. Mechanical characterization of fiber reinforced concrete with steel and polyester fiber. In: Proceedings of the BEFIB 2008, 7th RILEM international symposium on fibre reinforced concrete, Chennai, India. p. 537–46.
- [19] ACI Committee 544. Measurement of properties of fiber reinforced concrete. ACI report 544.2R-89. Farmington Hillis, Mich: American Concrete Institute. p. 1–11.
- [20] Buratti N, Mazzotti C, Savoia M. Post-cracking behaviour of steel and macro-synthetic fiber-reinforced concretes. *Constr Build Mater* 2011;25:2713–22.
- [21] Olivito RS, Zuccarello FA. An experimental study on the tensile strength of steel fiber reinforced concrete. *Composites: Part B* 2010;41:246–55.
- [22] UNI EN ISO 15630-1. Steel for the reinforcement and pre-stressing of concrete – test methods – Part 1: reinforcing bars, wire rod and wire. Italian Board of Standardization (UNI); 2010.
- [23] NTC 2008. Norme tecniche per le costruzioni. D.M. 14/01/2008 [in Italian].
- [24] UNI 9944 Corrosione e protezione dell'armatura del calcestruzzo. Determinazione della profondità di carbonatazione e del profilo di penetrazione degli ioni cloruro nel calcestruzzo. Italian Board of Standardization (UNI); 1992 [in Italian].
- [25] Collepardi M. Quick method to determine free and bound chlorides in concrete. In: RILEM international workshop on chloride penetration into concrete, Saint Remy-les-Chevreuse; 15–18 October 1995. p. 10–16.
- [26] Zerbino RL, Barragán BE. Long-term behavior of cracked steel fiber-reinforced concrete beams under sustained loading. *ACI Mater J* 2012;109:215–24.
- [27] Vasanelli E, Micelli F, Aiello MA, Plizzari G. Crack width prediction of FRC beams in short and long term bending condition. *Mater Struct* 2013. in press.
- [28] Vasanelli E, Micelli F, Aiello MA, Plizzari G. Mechanical and cracking behavior of concrete beams reinforced with steel bars and short fibers. *Stud Res* 2011;31:91–113.
- [29] FIB Model Code (2010). First complete draft. *fib Bull* 562010, vol. 2, ISBN 978-2-88394-096-3. p. 312 [Chapters 7–10].
- [30] Alahmad S, Toumi A, Verdier J, Francois R. Effect of crack opening on carbon dioxide penetration in cracked mortar samples. *Mater Struct* 2009;42:559–66.
- [31] Jana D, Erlin B. Carbonation as an indicator of crack age. *Concr Int* 2007;May:61–4.
- [32] Neville A. Can we determine the age of cracks by measuring carbonation? *Concr Int* 2004;January:88–91.
- [33] Liang MT, Qu WJ, Liao YS. A study of carbonation in concrete structures at existing cracks. *J Chin Inst Eng* 2000;223-2:143–53.